APTRA-based luminescent lanthanide complexes displaying enhanced selectivity for Mg^{2+}

Edward R. H. Walter, J. A. Gareth Williams* and David Parker*

Department of Chemistry, Durham University, South Road, Durham DH1 3LE, UK.

E-mail: ***david.parker@dur.ac.uk***, ***j.a.g.williams@durham.ac.uk***. Supporting information and ORCID(s) from the author(s) for this article are available on the www under ***http://dx.doi.org/10.1002/chem.***xxxxxxxxx

Abstract:

A series of three europium(III) complexes has been created in which an APTRA moiety has been integrated into the sensitising chromophore (APTRA = *o*-aminophenol-*N,N,N*-triacetate). The constitutionally isomeric complexes EuL^1 and EuL^2 feature the APTRA unit linked to a metal-bound pyridine ring through an alkynyl unit, differing according to the disposition of the APTRA substituents relative to the C≡C unit (*para*-N and *para*-O respectively). In EuL^3, the APTRA ring is directly bonded to the Eu-coordinated pyridine (*para*-O). The metal binding affinities for magnesium, calcium and zinc ions have been measured using emission and excitation spectroscopy. The pyridylalkynylaryl systems, EuL^1 and EuL^2, offer superior affinity and selectivity for Mg^{2+}. The Mg^{2+} affinities are surprisingly very different from prior studies on structurally related systems that incorporate organic fluorophores as reporters, as opposed to the macrocyclic Eu complex moiety. A much reduced affinity for calcium and zinc – possibly arising from the lower donor ability of the aryl N or O atoms arising from extended conjugation – means that magnesium ion concentrations can be measured directly in serum for the first time, using such an approach. An apparent dissociation constant for magnesium binding of K_d = 2.4 mM was calculated in the serum background.

Introduction

Luminescent lanthanide(III) complexes offer a number of fundamental advantages over alternative emissive probe systems. They possess large pseudo-Stokes' shifts, sharp emission bands that are characteristic of each lanthanide ion, and a fine structure in their emission spectra that is sensitive to the nature of the metal coordination environment. The Laporte and spin-forbidden nature of f-f transitions for many of the lanthanide(III) ions results in a long excited state lifetime (in the microsecond to milliseconds range), allowing time-gated measurements to be made. Such properties allow the lanthanide emission profile to be observed selectively, through the application of a short delay between excitation and spectral acquisition.[1,2] Lanthanide complexes require an aromatic chromophore or 'antenna' to 'sensitise' the emission, by absorbing light and transferring it to the excited state of the lanthanide ion, due to their low molar extinction coefficients.[3] The choice of the chromophore is an essential factor to consider when designing highly emissive lanthanide complexes for biological applications. The energy gap between the T_1 excited state of the chromophore and the Ln^{3+} excited states (Eu^{3+} $^5D_0$ = 17,200 cm^{-1}, Tb^{3+} $^5D_4$ = 20,400 cm^{-1})[1] must be small enough for energy transfer to occur efficiently but sufficiently large to avoid thermally activated repopulation of the T_1 from the long-lived lanthanide excited state.

A wide range of lanthanide complexes has been investigated examining affinity and selectivity towards both cations (K^+, Mg^{2+}, Ca^{2+}, Zn^{2+})[3-6] and anions (HCO_3^-, F^-).[7,8] In most instances, the chromophore structure includes the ion binding domain and a luminescence change occurring on binding of the target ion. To date, however, no luminescent lanthanide complexes that can bind magnesium selectively have been reported, due in part to the very slow progress made in devising magnesium-selective chelates.

Magnesium is the second most abundant cation in cells, with 'free' Mg^{2+} concentrations falling in the range of 0.8–1.5 mM.[9] It plays a fundamental role in a number of biological process in cells, acting as a co-factor in over 600 known enzymatic reactions,[10] and controlling the conformation of adenosine triphosphate (ATP), nucleic acids and proteins.[11] The *o*-aminophenol-*N,N,N*-triacetic acid (APTRA) unit is the most widely used binding chelate for magnesium in the literature, and has been incorporated into a range of luminescent systems.[12-15] Recently, it has

been successfully employed to provide evidence for Mg^{2+} fluctuations specific to the mitochondria, in the early stages of HeLa cell apoptosis.[16] APTRA chelates, however, possess a much higher affinity for Ca^{2+} over Mg^{2+}, restricting their application to the endo(sarco)plasmic reticulum, where Ca^{2+} concentrations are low.[17] Enhanced selectivity for Mg^{2+} has been achieved for a series of β-keto acid ligands,[18,19] but the low denticity of these systems gives rise to the formation of competing ternary adducts with nucleosides *in vivo*, limiting their direct biological application.[20]

Ligands that are able to bind magnesium in water with high selectivity over calcium are unknown. Some promising progress has been reported recently with the development of *o*-aminophenol-*N,N*-diacetate-*O*-methylene-methylphosphinate (APDAP), a new pentadentate phosphinate-based analogue of APTRA.[21,22] Using UV-visible absorption spectroscopy, APDAP has been shown to display a significantly enhanced selectivity for Mg^{2+}, as a consequence of a 110-fold reduction in affinity for Ca^{2+}.[21] The incorporation of the APDAP chelate into an alkynyl-naphthalene fluorophore has also enabled Mg^{2+} concentrations to be studied in a competitive binding environment.[22] Such behaviour suggests that the APDAP chelate has the potential to be used to monitor Mg^{2+} fluxes in regions of the body not previously explored, because of their elevated Ca^{2+} concentrations.[22]

APTRA-based luminescent lanthanide complexes that bind Mg^{2+} have been previously reported, albeit with significant competition from Ca^{2+} and Zn^{2+} ions. Reany, Parker and Gunnlaugsson, for example, developed APTRA chelates incorporated into a lanthanide-based system, e.g. **TbL^4** (**Figure 1**).[3,4] This complex displayed a low mM dissociation constant for Mg^{2+} but μM values for Ca^{2+} and Zn^{2+}.

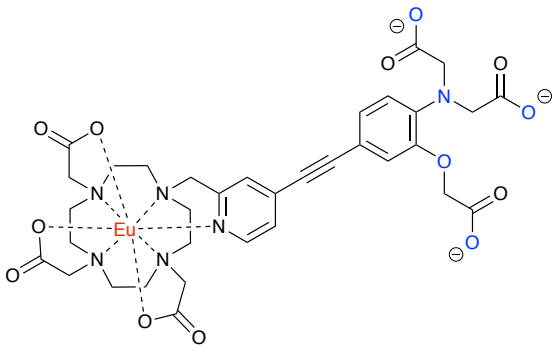

EuL[1]

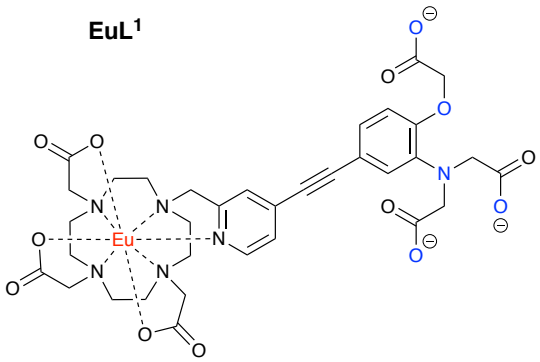

EuL[2]

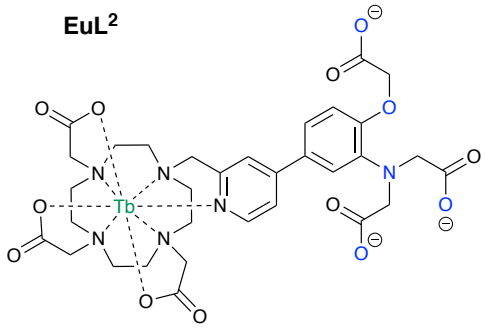

TbL[3]

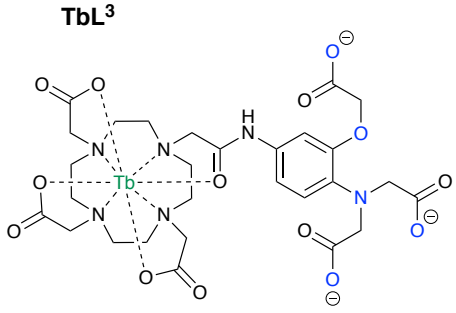

TbL[4]

Figure 1. Structures of **EuL[1]**, **EuL[2]**, **TbL[3]** and, for comparison, **TbL[4]**.[3,4]

Here, we report the synthesis of three new lanthanide complexes containing a pentadentate APTRA binding chelate (**Figure 1**). The complexes **EuL[1]** and **EuL[2]** are based upon a pyridylalkynyl chromophore and **TbL[3]** contains a bi-aryl chromophore to sensitise lanthanide emission. Comparisons of the cation affinity and selectivity profile for **EuL[1]** and **EuL[2]** are made here with the behaviour of the APTRA analogues containing an alkynyl-naphthalene fluorophore, recently reported in parallel work,[22]

and with the older **TbL^4** system.[3,4] The selection of these three new complexes allows the behaviour of systems with a pyridylalkynylaryl versus a bi-aryl chromophore to be compared, in order to assess the influence of the interannular linking unit on affinity, selectivity, and luminescence response to Mg^{2+}.

Results and Discussion

The lanthanide complexes containing an alkynylpyridyl chromophore **EuL^1 (Scheme 1)** and **EuL^2 (ESI, Scheme S.1)** were synthesised using similar procedures from the corresponding TIPS-protected alkynes **(1)** and **(5)**. The alkynylpyridyl chromophore was synthesised in a one-pot procedure involving alkyne de-protection with tetrabutylammonium fluoride (TBAF) and a palladium-catalysed cross-coupling reaction with 4-bromo-2-(hydroxymethyl)pyridine. Compound **(2)** was formed in moderate yield, and the alcohol was converted to the benzylic bromide with phosphorus tribromide in dichloromethane to give **(3)** in quantitative yield. Alkylation of the ethyl ester of DO3A with **(3)** was achieved in anhydrous acetonitrile at 60 ^oC using caesium carbonate as the base. Base-catalysed ester hydrolysis, followed by reaction with $EuCl_3.6H_2O$ at pH 5.5, gave rise to **EuL^1**, which was purified *via* reverse-phase HPLC using an ammonium carbonate and acetonitrile buffered system.

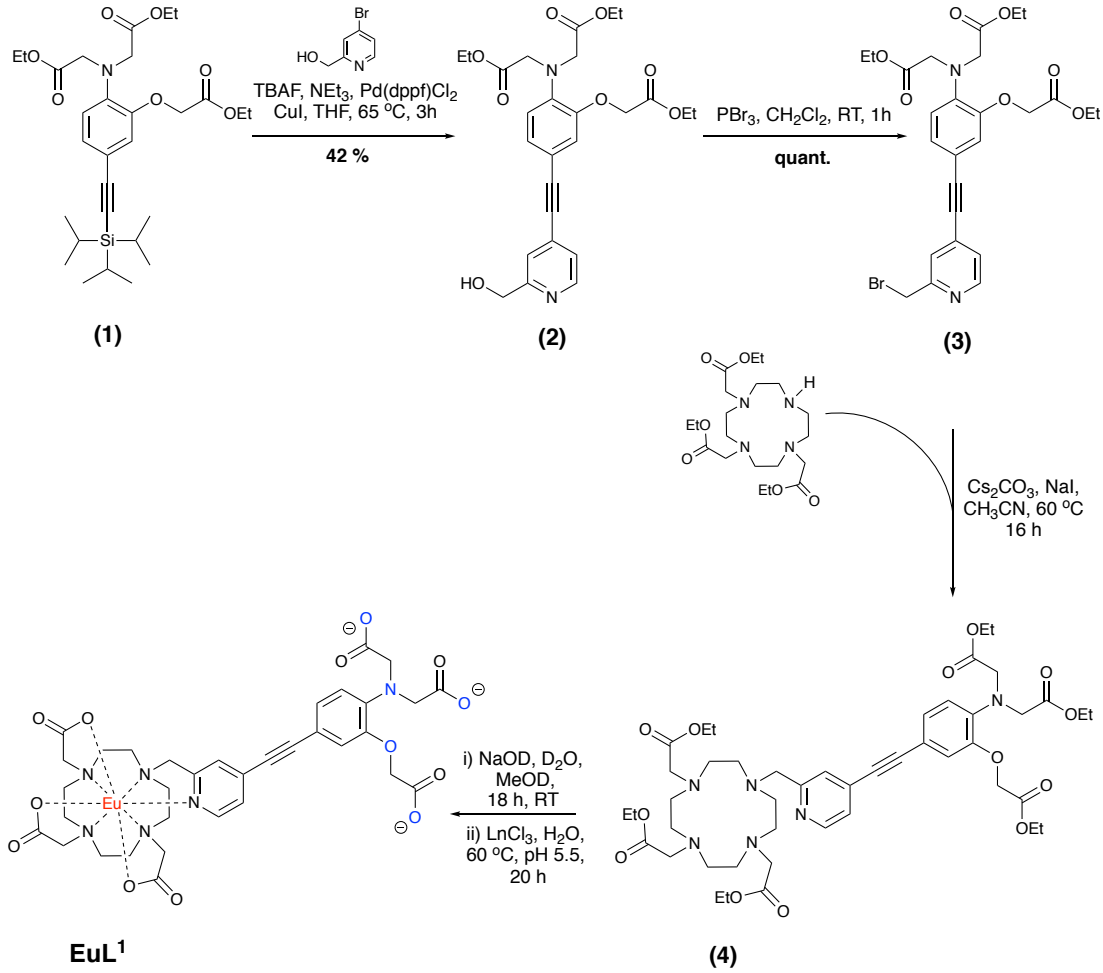

Scheme 1 Synthesis of **EuL^1**.

The bi-aryl complex, **TbL^3**, was synthesised in a multi-step reaction sequence, as reported recently in parallel work that also defined the effect of solvent polarity and oxygen sensitivity on the terbium luminescence emission behaviour.[23]

Photophysical studies of EuL^1, EuL^2 and TbL^3

The photophysical properties of the complexes **EuL^1**, **EuL^2** and **TbL^3** were studied in aerated aqueous solution at 298 K, and are summarised in **Table 1**. The absorption spectrum of **EuL^1** (**Figure 2**) displays three maxima; the bands at 270 nm and 315 nm are attributed to localised π–π* excited states, with the broad structureless band at 380 nm assigned to an intramolecular charge-transfer (ICT) transition within the pyridylalkynylaryl chromophore. Intense europium-based emission was observed following excitation into the π–π* transition at 315 nm, whilst excitation into the ICT band gave rise to weak Eu^{3+} emission at room temperature. Similarly, **EuL^2** displays a structured π–π* band at 315 nm that sensitises europium-based luminescence. The ICT transition at 360 nm is significantly blue-shifted and less pronounced than

that of **EuL^1**, reflecting the poorer electron donating ability of the *para* phenolic oxygen atom. The absorption spectrum of the bi-aryl complex **TbL^3** has a maximum at 280 nm assigned to a localised π–π* excited state, and was earlier shown to exhibit solvatochromic behaviour.[23] As with **EuL^2**, the weak shoulder at lower energy (340 nm) is probably associated with an ICT transition.

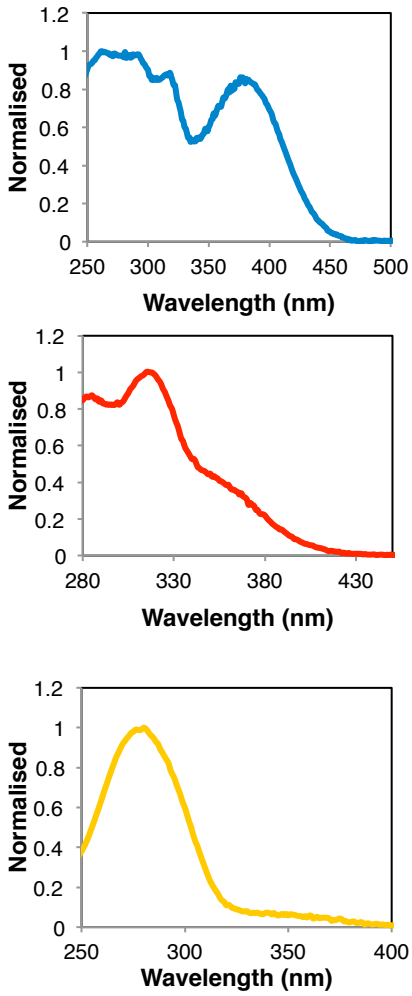

Figure 2. Normalised absorption spectra of **EuL^1** (*blue*), **EuL^2** (*red*) and **TbL^3** (*orange*); (H_2O, 298 ± 3 K).

Table 1. Photophysical data for **EuL[1]**, **EuL[2]** and **TbL[3]** (298 ± 3 K); lifetimes are given in milliseconds, estimated uncertainty ± 10%. Quantum yields (**Φ**) ± 20 % measured in H_2O.

	EuL[1]	**EuL[2]**	**TbL[3]** [23]
λ_{abs} / nm (ε / M^{-1} cm^{-1}) [a]	270 (12000)	315 (18400)	280 (6000)
	315 (10499)	360 (6700)	345 (200)
	380 (11500)		
$\tau(H_2O)$	0.61	0.65	0.43, 1.52 [b]
$\tau(D_2O)$	1.87	1.89	0.72, 2.30 [b]
$\tau(H_2O)$ (Mg^{2+} sat.)	0.59 [d]	0.59 [d]	0.64 [e]
$\tau(D_2O)$ (Mg^{2+} sat.)	1.61 [d]	1.70 [d]	-
$\Phi(H_2O)$ / %	13.0 [f]	11.0 [f]	5.4 [b,g]

[a] In H_2O. [b] Determined under degassed conditions; europium lifetimes were not sensitive to deoxygenation [c] The hydration number, *q*, is 1 for each complex and is independent of complex concentration. [d] Lifetime after the addition of 40 mM Mg^{2+}. [e] Lifetime after the addition of 200 mM Mg^{2+}. [f] Quantum yield measured using $[Ru(bpy)_3]Cl_2$ in water as the standard (Φ = 0.028).[24] [g] Quantum yield measured using quinine sulphate in 0.5 M $H_2SO_{4\,(aq)}$ as the standard (Φ = 0.55).[25].

Influence of protonation and determination of pK_a

A study into the effect of pH on the absorption and emission spectra of complexes containing both a pyridylalkynylaryl and a bi-aryl chromophore was carried out in aqueous solution. Calculated pK_a values from the titrations are shown in **Table 3**, with the value reported for **TbL[4]** provided for comparison.

Table 2. The calculated pK_a values of **EuL[1]**, **EuL[2]** and **TbL[3]** (100 mM KCl, 298 K); the error associated with the fitting is given in parenthesis. The pK_a value for **TbL[4]** is provided for comparison.

Complex	**pK_a**
EuL[1]	4.5(02) [a]
EuL[2]	6.7(04) [b]
TbL[3]	[c]
TbL[4]	6.4 [b 3,4]

[a] determined by absorption spectroscopy ; [b] determined by emission spectroscopy; [c] no significant pH response was observed in absorption or emission.

The pK_a of **EuL[1]** was calculated from absorption spectroscopy measurements **(Figure S.1)**. No pH sensitivity was observed in the emission spectrum over the pH range 4 to 8. In basic solution, the absorption spectrum of **EuL[1]** displays three maxima at 270 nm, 315 nm and 378 nm, in a profile identical to that shown (**Figure**

2). Following addition of acid, a 15 nm hypsochromic shift of the ICT band from 378 nm to 363 nm was observed, with an isosbestic point at 370 nm (ESI, **Figure S1**). The hypsochromic shift is attributed to protonation of the aniline nitrogen atom under acidic conditions. No pronounced changes in absorbance were found in either the 270 nm or 315 nm bands at lower pH. A pK_a value of 4.5 was calculated from the ratio of the λ_{max} of the deprotonated and protonated forms.

The absorption spectra measured for **EuL^2** were insensitive to pH for both the π–π^* and ICT transitions. A pK_a value of 6.7 could, however, be calculated using emission spectroscopy, where a 2.2-fold reduction in intensity was observed across the pertinent pH range (ESI **Figure S2**). No pK_a value could be estimated for the bi-aryl complex **TbL^3**, as both its absorption and emission spectra were insensitive to pH (ESI **Figure S3**).

Metal ion binding studies with EuL^1, EuL^2 and TbL^3

Binding monitored using absorption spectroscopy

EuL^1 In the 'metal-free' state, the absorption spectrum of **EuL^1** is as shown in **Figure 2**. Following addition of metal ions, an increase in absorbance was observed at the π–π^* band and a decrease in the ICT band. An isosbestic point is observed at 345 nm for Mg^{2+} and 339 nm for Ca^{2+} and Zn^{2+} (**Figure 3**).

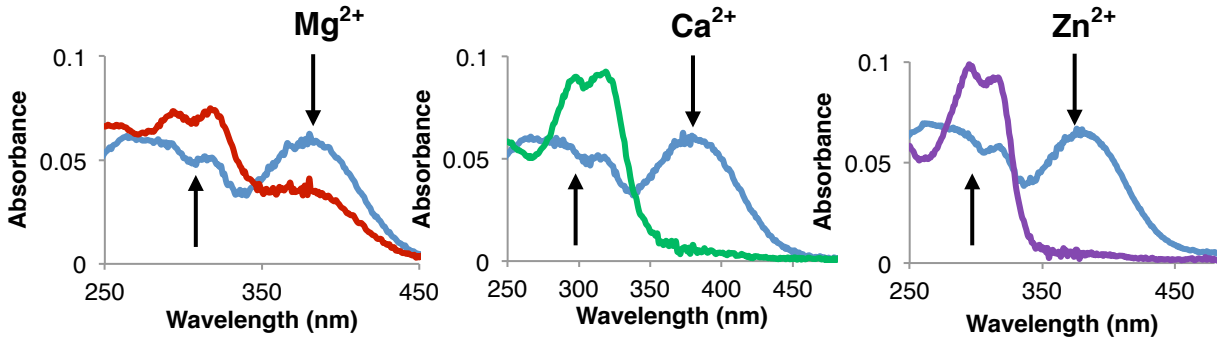

Figure 3. Absorption spectra for **EuL^1** (blue) and following addition of **(A)** Mg^{2+} (150 mM) (red), **(B)** Ca^{2+} (15 mM) (green) and **(C)** Zn^{2+} (35 μM) (purple). **[EuL^1]** = 5 μM , 50 mM HEPES, 100 mM KCl, pH 7.21, 298 K.

It is apparent from analysis of **Figure 3**, that following addition of Ca^{2+} and Zn^{2+} to **EuL^1**, the ICT state at 380 nm is perturbed, with the complete disappearance of the ICT band upon saturation with the added metal. With Mg^{2+}, however, a different spectral response was observed, with only a 1.6-fold decrease in the ICT transition intensity. This differing behaviour suggests that the *para* aniline nitrogen atom plays a much more important role in the binding of Ca^{2+} and Zn^{2+} than for Mg^{2+}.

EuL^2 The absorption spectrum of **EuL^2** displays an absorption band at 315 nm in both the 'metal-free' and 'bound' states. A 1.1-, 1.3- and 1.5-fold increase in absorbance was observed at 315 nm, following addition of Mg^{2+}, Ca^{2+} and Zn^{2+} ions respectively (**Figure 4**). Similarly to **EuL^1**, the perturbation of the ICT state at 368 nm gave rise to an isosbestic point centred at 343 nm.

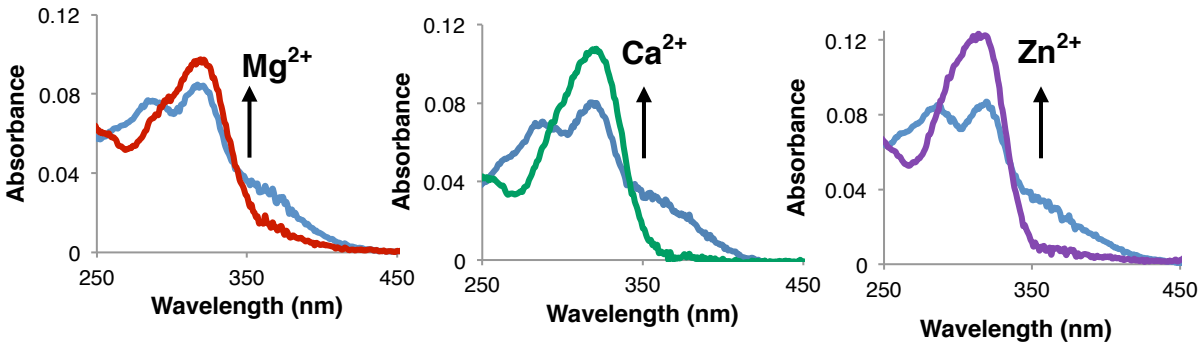

Figure 4. Absorption spectra of **EuL^2** for the addition of **(A)** Mg^{2+} (20 mM) (red), **(B)** Ca^{2+} (3.5 mM) (green) and **(C)** Zn^{2+} (11 μM) (purple).
[EuL^2] = 5 μM in 50 mM HEPES, 100 mM KCl, pH 7.21, 298 K.

TbL^3 The bi-aryl complex **TbL^3** displays a λ_{max} at 280 nm **(Figure 2)**. Following addition of divalent metal ions, a slight increase in absorbance at this wavelength was observed. For example, after the addition of Mg^{2+}, a 1.2-fold increase was observed (**Figure S.4**, **ESI**).

Luminescence binding studies

EuL^1 The emission spectra of **EuL^1** following the addition of Mg^{2+} and Ca^{2+} are shown in **Figure 5**, displaying a 1.5- and 1.8- fold reduction in the total emission intensity respectively. The addition of Zn^{2+}, however, resulted in a 1.8-fold enhancement in the total emission intensity (**ESI**, **Figure S5**). Dissociation constants of 7.5 mM, 0.9 mM and 1.8 μM were calculated following the addition of Mg^{2+}, Ca^{2+} and Zn^{2+} respectively.

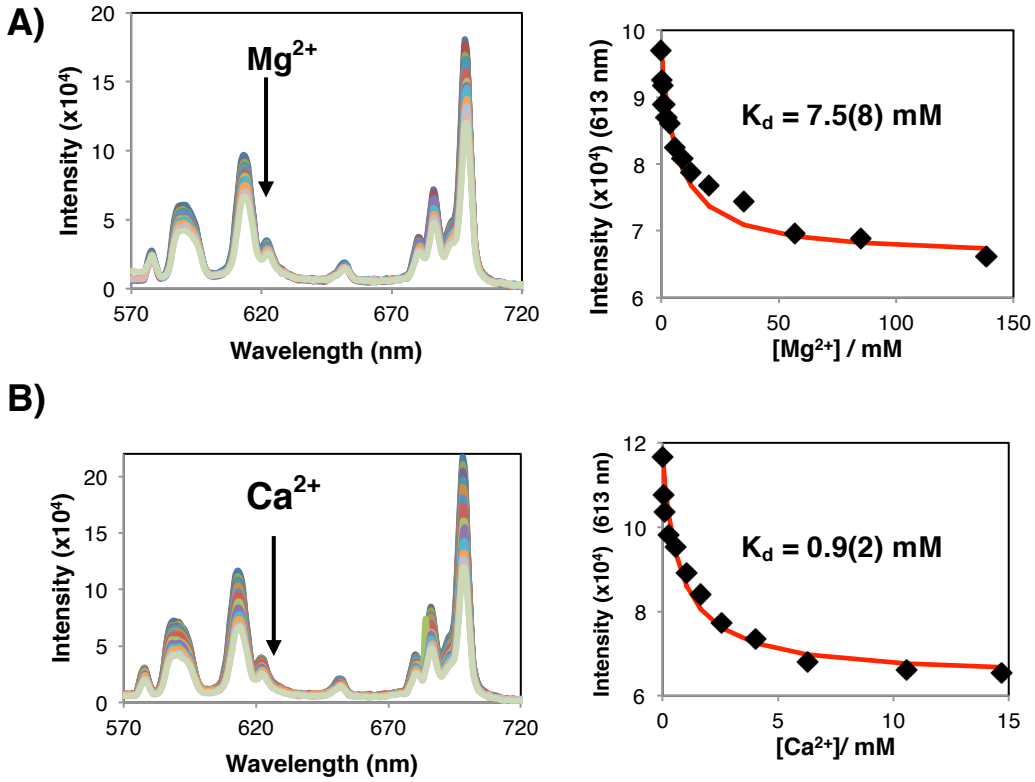

Figure 5 (Left) emission spectra; (right) fitting of the emission intensity against the added concentration of **(A)** Mg^{2+} and **(B)** Ca^{2+} to a 1:1 binding model. [**EuL^1**] = 5 μM in 50 mM HEPES, 100 mM KCl, pH 7.21, 298 K; λ_{ex} = 339 nm. The reported dissociation constants are an average of two separate metal ion titrations, and are given with the experimental error in parenthesis.

The excitation spectrum of **EuL^1** displayed two maxima at 287 and 314 nm. The band at 380 nm in the absorption spectrum associated with conjugation of the *para* aniline nitrogen lone pair into the chromophore was not evident in the excitation spectrum. Typical of luminescent N-*para*-substituted APTRA analogues in the literature,[12-15] an excitation-based ratiometric response was observed after binding to divalent metal ions Mg^{2+}, Ca^{2+} and Zn^{2+} (*ESI,* **Figure S6**). Comparable K_d values, close to being within the experimental error for the measurement, were obtained in each case.

EuL^2 In contrast to the emission spectral response observed for **EuL^1**, the addition of Mg^{2+}, Ca^{2+} (**Figure 6**) and Zn^{2+} (*ESI*, **Figure S7**) resulted in a 1.4-, 2.5-, and 6-fold

enhancement in the luminescence emission intensity. A non-ratiometric excitation response was reported for **EuL^2**, in accordance with the structurally comparable naphthalene systems containing an aniline nitrogen atom *meta* to the chromophore.[22]

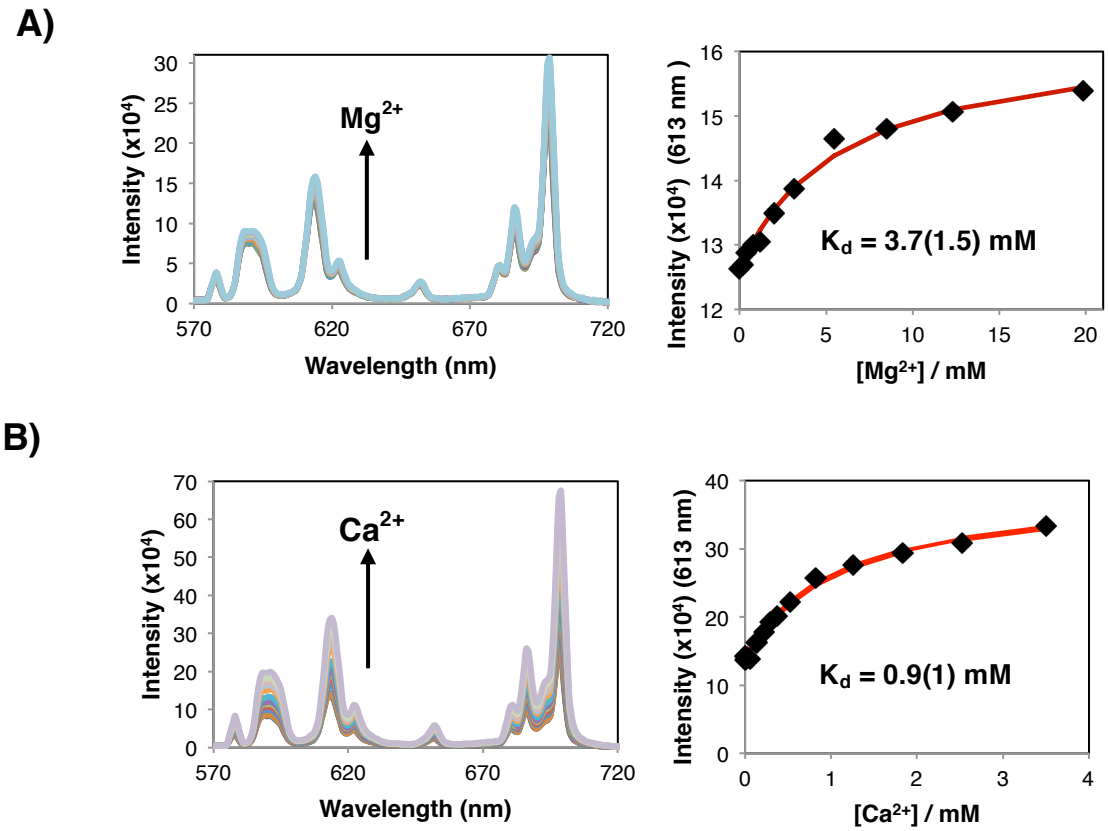

Figure 6. (Left) emission spectra; (right) fitting of the emission intensity against the added concentration of **(A)** Mg^{2+} and **(B)** Ca^{2+} to a 1:1 binding model. [**EuL^2**] = 5 μM in 50 mM HEPES, 100 mM KCl, pH 7.21, 298 K; λ_{ex} = 343 nm. The reported dissociation constants are an average of two separate metal ion titrations, and are given with the experimental error in parenthesis.

Dissociation constants of 3.7 mM, 0.9 mM and 1.9 μM for the binding of Mg^{2+}, Ca^{2+} and Zn^{2+} were calculated respectively, and are comparable to those of **EuL^1**. A slightly higher affinity towards Mg^{2+} is seen for **EuL^2**, which is likely to be due to the *meta* aniline nitrogen atom playing a more prominent in binding.

It is evident that both **EuL^1** and **EuL^2**, incorporating the pyridylalkynylaryl chromophore, do not display a ratiometric response involving the hypersensitive ΔJ = 2 and ΔJ = 4 emission bands. In each case, only the total emission intensity change is reported (*ESI*, **Figure S8**). Along with the fact that there are negligible changes in the luminescence lifetime measurements of **EuL^1** and **EuL^2** following Mg^{2+} binding

(**Table 1**), these observations indicate that the coordination environment of the europium centre is largely unaffected by the binding of divalent metal ions.

TbL^3 Binding studies of the system containing a bi-aryl pyridylaryl chromophore were undertaken with **TbL^3** rather than **EuL^3**, due to a more efficient energy transfer arising from the triplet excited state of the chromophore to the $^5D_4$ excited state of Tb^{3+}. The study set out to examine whether the use of a bi-aryl as opposed to ethynyl-based chromophore would change the selectivity and affinity for divalent metal ions. The binding studies were examined with the bi-aryl APTRA binding chelate incorporating a *meta* aniline nitrogen, as it was found that **EuL^2** (with *meta* aniline nitrogen) displayed a higher affinity for Mg^{2+} compared to **EuL^1**, while maintaining almost identical affinities for Ca^{2+} and Zn^{2+}.

The emission spectra following addition of Mg^{2+}, Ca^{2+} are shown in **Figure 7**, displaying a 2.6-fold and 2.5-fold reduction in the emission intensity of the $^5D_4 \rightarrow {}^7F_5$ band at 544 nm, respectively. Similarly to **EuL^1**, the addition of Zn^{2+} (**ESI**, **Figure S9**) produced a quite different response, with a 1.8-fold increase in the emission intensity. Dissociation constants of 17 mM, 0.8 mM and 0.5 μM were calculated for the binding of Mg^{2+}, Ca^{2+} and Zn^{2+} respectively.

Interestingly, in contrast to **EuL^1** and **EuL^2** a linear dependence between the luminescence lifetime of the $^5D_4$ excited state of Tb^{3+}, and the concentration of Mg^{2+} was found (**Figure 8**). Under aerated conditions, a 1.4-fold increase in the lifetime was calculated, following addition of up to 200 mM Mg^{2+}.

A)

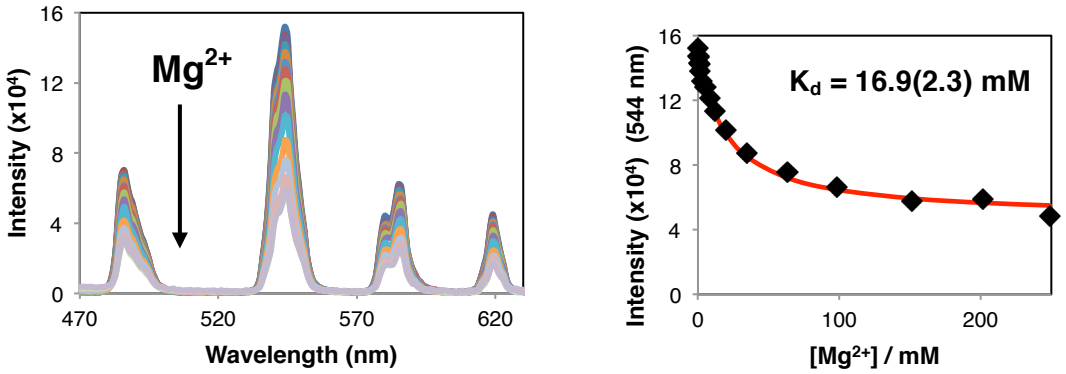

B)

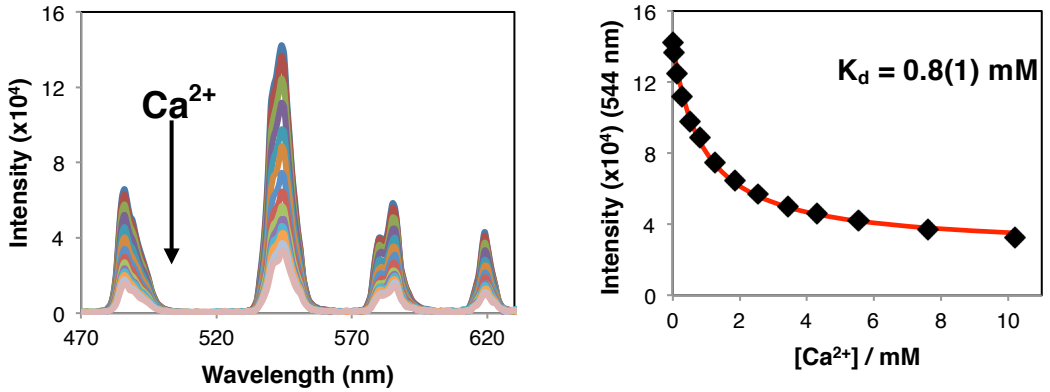

Figure 7. (Left) emission spectra for **TbL^3**; (right) fitting of the emission intensity variation with concentration of **(A)** Mg^{2+} and **(B)** Ca^{2+} , assuming a 1:1 binding model. [**TbL^3**] = 5 μM in 50 mM HEPES, 100 mM KCl, pH 7.21, 298 K; λ_{ex} = 280 nm. The reported dissociation constants are an average of two separate metal ion titrations, and are given with the experimental error in parenthesis.

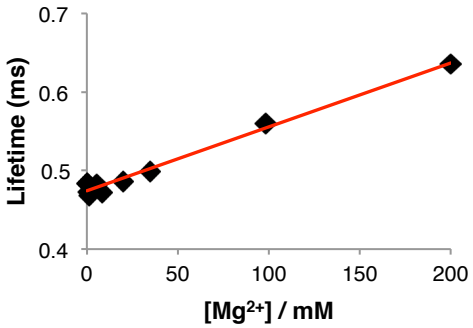

Figure 8. The linear dependence of the $^5D_4$ excited state lifetime of **TbL^3** on the concentration of Mg^{2+}. [**TbL^3**] = 5 μM in 50 mM HEPES, 100 mM KCl, pH 7.21, 298 K; λ_{ex} = 280 nm.

In our previous work, the excited state lifetime of **TbL^3** was found to be sensitive to changes in solvent polarity and the presence of dissolved oxygen in solution. [23] Polar solvents such as water stabilised the excited state via dipolar interactions, reducing its luminescence lifetime. It is tempting to speculate, therefore, that the binding of Mg^{2+} may cause a destabilising effect on the triplet excited state structure due to a reduction in complex hydration, and thereby reduces the extent to which oxygen quenches, thus increasing the emission lifetime. In contrast, the europium-based analogue **EuL^3** showed no significant change in excited state lifetime following addition of 200 mM Mg^{2+}. A change of 0.5 ms to 0.43 ms was observed in aerated aqueous solution, within the error associated with the lifetime measurement.

Discussion: pyridylalkynylaryl versus pyridylaryl chromophores

The use of a bi-aryl chromophore instead of the pyridylalkynylaryl chromophore presents a number of disadvantages for magnesium-sensing applications. Although a similar affinity is observed for the binding of Ca^{2+} and Zn^{2+}, a weaker binding affinity for Mg^{2+} was found. For example, a 4.5-fold reduction in the affinity was seen relative to **EuL^2** (**Table 3**). The high-energy excitation required for the less conjugated bi-aryl complex **TbL^3**, also limits its possible biological applications in its current state. Its use *in vivo* and *in cellulo* is restricted, as confocal microscopy experiments for the visualisation in cells typically require λ_{ex} = 355 nm or longer.[26,27] The introduction of methoxy groups *ortho* to the chromophore could be undertaken in future, in order to red-shift the absorption band λ_{max} value.

Table 3. The calculated dissociation constants of **EuL^1**, **EuL^2, TbL^3** and **TbL^4** via emission spectroscopy (50 mM HEPES, 100 mM KCl, pH 7.21, 298 K). The reported binding constants following the addition of Mg^{2+}, Ca^{2+} and Zn^{2+} are from an average of two independent metal ion titrations, and are given with the experimental error in parenthesis.

Complex	Mg^{2+}		Ca^{2+}		Zn^{2+}	
	Log K	K_d / mM	Log K	K_d / mM	Log K	K_d / μM
EuL^1	2.1(1)	7.5(8)	3.0(1)	0.9(2)	5.7(2)	1.8(5)
EuL^2	2.4(2)	3.7(1.5)	3.0(1)	0.9(1)	5.7(1)	1.9(1)
TbL^3	1.8(1)	17(2)	3.1(1)	0.8(1)	6.3(1) [a]	0.5(2) [a]
TbL^4	3.2 [b]	0.8 [b]	4.1 [b]	0.05 [b]	5.0 [b]	10.5 [b]

[a] Binding titration was not repeated; the reported error is associated with the fitting. [b] Values calculated by Parker *et al.*[3,4]

Discussion: comparison of the binding affinity and selectivity of EuL[1], EuL[2] and TbL[3] with literature APTRA analogues

Lanthanide complexes **EuL[1], EuL[2]** and **TbL[3]** each display mM affinities for Mg^{2+} and Ca^{2+}, and a low μM affinity for Zn^{2+}. The position of the aniline nitrogen atom relative to the chromophore has been shown to have no significant effect on the affinity or selectivity towards the divalent metal ions studied.

From the analysis of the calculated dissociation constants (**Table 3)**, it is apparent that the lanthanide-based APTRA complexes display a much lower affinity for Ca^{2+} than their analogues.[12-15] The significant improvement in the Mg^{2+} / Ca^{2+} selectivity displayed here is extremely rare, and has never been reported previously for ligands and complexes of this type. In each literature example, pentadentate carboxylate-based APTRA indicators have an enhanced selectivity towards Ca^{2+}, with a typical affinity in the low- to mid-μM range in aqueous solution.[12-15] For example, **EuL[2]** displays an 18-fold reduced affinity for Ca^{2+} binding compared to the **TbL[4]** complex developed by Reany, Parker and Gunnlaugsson,[3] and a 23-fold reduction in relation to the APTRA-based alkynylnaphthyl series reported in our own previous work.[22] The lower affinity observed for Ca^{2+} binding may be due in part to the lower donor ability of the aryl N and O atoms, associated with the strong internal charge transfer present in these pyridyl-alkynylaryl systems. The effect is most pronounced when the pyridine N is coordinated to the lanthanide ion that acts as a charge sink. It is also possible that differential solvation effects may partly account for the changes in selectivity. The relative solvation of both the host Eu complex/ligand and the group 2 cation will influence the overall free energy of complexation.[28] For example, Riis-Johannessen *et al.* highlighted how predictions based on Coulombic repulsion between lanthanide and transition metal ions can be overturned in polymetallic systems owing to simultaneous increases in solvation energy as the net charge increases.[29]

Irrespective of the physiochemical origins of the difference in selectivity, such cation selectivity profiles present an opportunity to use the lanthanide complexes synthesised in this study to monitor the flux of 'free' Mg^{2+} concentrations in calcium-rich samples. Serum is just such a medium: no studies of magnesium binding using luminescent probes have previously been reported in serum.

Applications of EuL^2: assessing 'free' Mg^{2+} in newborn calf serum

Lanthanide complexes have been used to sense several bioactive species in biological fluids.[30-32] Europium- and terbium-based complexes containing an azaxanthone sensitiser, for example, have been utilised as probes for bicarbonate anions in human serum.[30] Measuring selectively the 'free' concentration of Mg^{2+} within human serum is of a major interest, as the onset of hypermagnesemia and hypomagnesaemia has been regularly linked to a wide range of chronic diseases.[33,34] To date, however, no APTRA-based ligand or complex has been used to monitor 'free' Mg^{2+} concentrations in human serum, due to the much higher affinity for Ca^{2+} ions.

Here, lanthanide-based APTRA complexes have shown encouraging results in metal ion binding titrations, with a low mM affinity for both Mg^{2+} and Ca^{2+} and a low μM affinity for Zn^{2+}. The increased selectivity for Mg^{2+} in this series presents an opportunity to study the binding of divalent metal ions in a competitive medium, such as newborn calf serum (NCS). The complex **EuL^2** was chosen over **EuL^1** for two reasons. First, **EuL^2** displayed the highest affinity for Mg^{2+} in the pyridylalkynylaryl chromophore series, with a calculated dissociation constant of 3.7 mM, and second, a more attractive 'turn-on' emission response occurs in response to Mg^{2+} binding.

The emission spectra of **EuL^2** in NCS are shown in **Figure 9**, with excitation at both λ_{max} in the 'un-bound' state (315 nm) and at the isosbestic point (343 nm) determined in a non-competitive background of HEPES buffer. The europium-centred emission was sufficiently bright at both excitation wavelengths that no time gating emission was required to remove short-lived fluorescence. However, the total emission intensity and excited state lifetime of **EuL^2** in NCS was significantly lower than that in HEPES buffer. In NCS, for example, the excited state lifetime of **EuL^2** was 0.3 ms in both the metal 'free' and 'bound' states. Such behaviour can be attributed to a quenching effect of amino-acid residues like tyrosine that are present in serum proteins (*e.g.*, bovine serum albumin) (**ESI**, **Figure S10**), and the presence of other electron-rich species in NCS that may quench the intermediate ligand excited state.

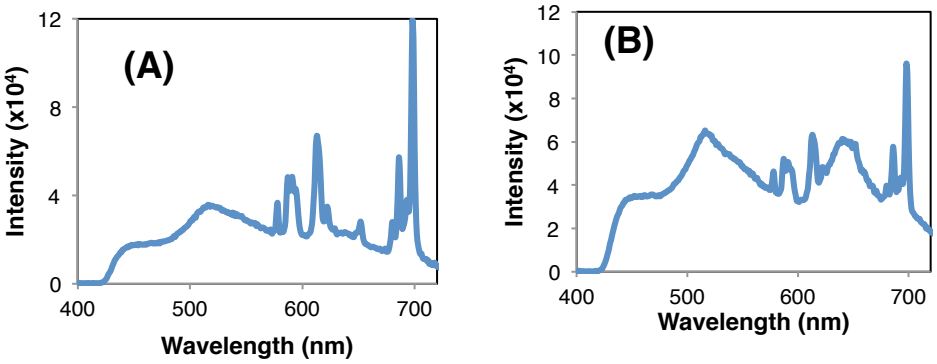

Figure 9. The emission spectrum of **EuL^2** in NCS (in which the concentrations of K^+, Ca^{2+} and Mg^{2+} are 3.9 mM, 2.6 mM and 0.8 mM respectively, as determined by ICP-OES). **(A)** λ_{ex} = 315 nm and **(B)** λ_{ex} = 346 nm, 298 K. [**EuL^2**] = 5 μM.

The change of the emission spectrum upon addition of Mg^{2+} in NCS is shown in **Figure 10**. From ICP-OES measurements, it was determined that there was a background concentration of 2.6 mM Ca^{2+}, 0.8 mM Mg^{2+} and 3.9 mM K^+ prior to the Mg^{2+} titration. Following addition of a further 100 mM Mg^{2+}, a 1.3-fold decrease in the emission intensity at the $\Delta J = 2$ transition at 613 nm was observed.

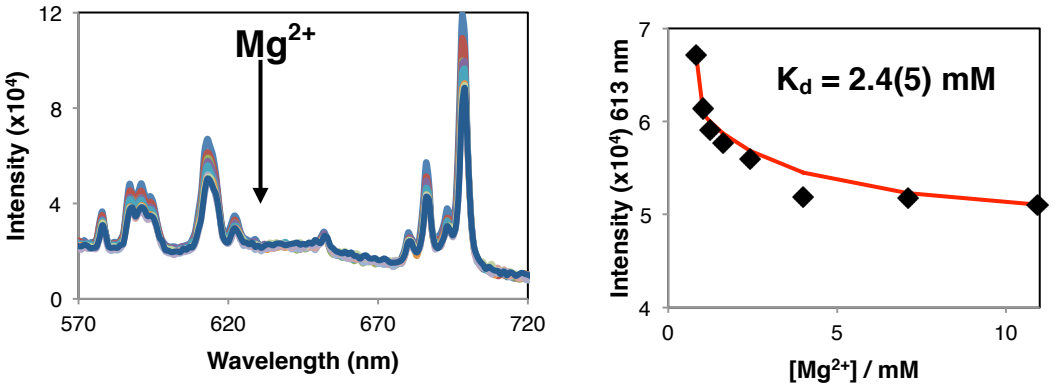

Figure 10. (Left) The emission spectrum of **EuL^2** in NCS (with metal content as in caption to Fig. 9) following the addition of Mg^{2+}. (Right) the fitting of the emission intensity against the concentration of Mg^{2+} to a 1:1 binding model. [**EuL^2**] = 5 μM, λ_{ex} = 315 nm, 298 K.

In buffered aqueous solution, an increase in emission intensity had been observed in response to Mg^{2+} binding (**Figure 6**). The observation of a decrease in the intensity with addition of Mg^{2+} for the complex in NCS can be attributed to the presence of a significant amount of Ca^{2+}-bound EuL^2. It can be seen from Figure 6 that Ca^{2+} leads to a larger increase of the emission intensity than Mg^{2+}, and so the decrease observed in NCS reflects the competitive displacement of Ca^{2+} by Mg^{2+}. A dissociation constant of 2.4 mM was estimated from the variation of the emission intensity at 613 nm, at both excitation wavelengths studied. Similarly to the non-

competitive binding environment in HEPES buffer, a non-ratiometric response was observed in the emission spectrum, with no change in the coordination environment of the europium ion on Mg^{2+} binding. A K_d value in the low mM range suggests that **EuL^2** and its congeners have the potential to detect fluxes of 'free' Mg^{2+} in biological media, such as serum.

Summary and Conclusions

The synthesis and photophysical studies of new lanthanide-based APTRA complexes containing both pyridylalkynylaryl and the related bi-aryl chromophores have been reported. Each of the complexes **EuL^1**, **EuL^2** and **TbL^3** was found to have emission intensities that were insensitive to pH in the physiological range, and displayed an enhanced selectivity towards Mg^{2+} ions compared to APTRA derivatives previously discussed in the literature. The K_d values reported for Ca^{2+} are all in the low mM range, compared with the low to mid-μM range typically observed for pentadentate APTRA analogues, such as **TbL^4**, and the series of naphthyl derivatives described by us recently.[22] Complexes containing the pyridylalkynylaryl chromophore are preferred for the highest affinity and selectivity for Mg^{2+} ions, and offer greater possibilities for future intracellular binding studies, because of their higher energy excitation wavelengths. Similar to the alkynyl naphthalene systems,[22] the position of the aniline nitrogen atom in relation to the chromophore had a minimal effect on the affinity and selectivity towards the divalent cations tested. In common with literature APTRA sensors, the excitation spectrum for **EuL^1** displayed a ratiometric response, following addition of Mg^{2+}, Ca^{2+} and Zn^{2+}.

The reduced binding affinity observed for Ca^{2+} in non-competitive media allowed the binding of Mg^{2+} to be investigated in neonatal calf serum (NCS). The study carried out with **EuL^2** is, to our knowledge, the first reported APTRA-based ligand or complex developed that has been used to monitor 'free' Mg^{2+} fluxes in serum. Encouraging results were obtained in NCS following the addition of Mg^{2+}. A dissociation constant of 2.4 mM was calculated, suggesting that sensors of this type could be used to study fluctuations in the concentration of 'free' Mg^{2+} in human serum.

Experimental

General procedures

All commercially available reagents were used as received from suppliers, without further purification. All moisture sensitive reactions were carried out under Schlenk-line techniques. Thin-layer and column chromatography was performed on silica (Merck Art 5554) and visualised under UV irradiation (254 nm). Routine ^{1}H (400 MHz) and ^{13}C (101 MHz) and ^{31}P (162 MHz) NMR spectra were acquired on Varian Mercury 400 NMR spectrometers. ^{13}C NMR and ^{31}P NMR spectra were run on a proton decoupled experiment. Two-dimensional NMR spectra (COSY, HSQC and HSBC) were run on Varian-600 (600 MHz) or VNMRS-700 (700 MHz) instruments. ES-MS data was acquired on a Waters TQD mass spectrometer interfaced with an Acquity UPLC system. Mass spectra of lanthanide complexes were recorded on a Waters Xevo QToF instrument in an acetonitrile and ammonium bicarbonate buffered (25 mM) system.

pK_a Determination

pH measurements were recorded using a Jenway 3510 pH meter in combination with a Jenway 924 005 pH electrode. The pH probe was calibrated before each independent titration using buffer solutions of pH 4, 7 and 10. Samples were prepared with a background of constant ionic strength (I = 0.1 M KCl, 298 K), and titrated to acid. The resulting sigmoidal curve of fluorescence intensity vs. pH was fitted by a non-linear least squares iterative analysis by Boltzmann using Origin 8.0 software. pK_a values were calculated with an error associated with the fitting.

Metal ion binding studies

All divalent metal binding studies for the addition of Mg^{2+}, Ca^{2+} and Zn^{2+} ([M^{2+}]) were carried out in buffered solutions of 50 mM HEPES and 100 mM KCl maintained at pH 7.2. All titrations were run in aqueous solution, with water purified by the 'Purite$_{STILL}$plus' system with a conductivity of $\leq$0.04 μS cm^{-1}. Stock solutions of [M^{2+}] were prepared containing the same concentration of the sensor used in the titration to avoid sample dilution. Absorption, emission and excitation spectra were run 5 min after the addition of small aliquots of [M^{2+}] to ensure the sample had fully equilibrated. Dissociation constants (K_d values) for the binding of Mg^{2+} and Ca^{2+} were generated from a 1:1 binding model obtained from a least squares fitting iterative from *www.supramolecular.org*.[35] In the case of Zn^{2+} binding, K_d's were calculated from a

1:1 binding model from **Equation S3** and **Equation S4** (see **ESI** for more information). Errors associated with the K_d values were generated from two or more repetitions of the binding experiments.

Ligand synthesis

Compound **(1)** was synthesised in a three-step procedure from 2-aminophenol, as described elsewhere.[22]

Diethyl 2,2'-((2-(2-ethoxy-2-oxoethoxy)-4-((2-(hydroxymethyl) pyridine-4-yl) ethynyl)phenyl)azanediyl)diacetate, (2)

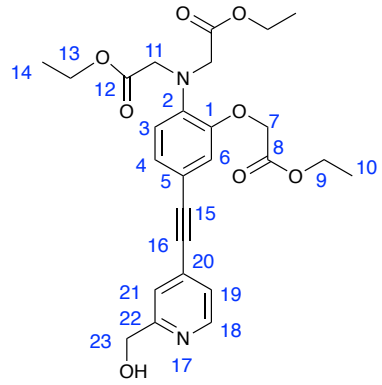

Compound **(1)** (973.0 mg, 1.80 mmol) and 4-bromo-2-(hydroxymethyl) pyridine (310.7 mg, 1.66 mmol) were dissolved in anhydrous THF (8 mL) and the solution was degassed by three freeze-pump-thaw cycles. Triethylamine (4.8 mL), $Pd(dppf)Cl_2$ (132.4 mg, 0.018 mmol) and CuI (110.6 mg, 0.58 mmol) were then added and the solution was degassed once more. Tetrabutylammonium fluoride (TBAF, 1 M solution in THF, 0.5 mL, 0.5 mmol) was then added before the brown solution was degassed with three final freeze-pump-thaw cycles. The reaction mixture was stirred at 65°C for 3 h under argon, before the solvent was removed under reduced pressure to form a dark brown / black residue. Purification by column chromatography (gradient hexane to ethyl acetate (with 1 % triethylamine)) afforded a yellow / brown oil (580 mg, 65 %). ^{1}H NMR (700 MHz, $CDCl_3$,) 8.53 (1 H, br s, H^{18}), 7.29 – 7.69 (2 H, br m, H^{19} and H^{21}), 7.12 (1 H, dd, *J* 9, 2, H^4), 6.94 (1 H, d, *J*, 2, H^6), 6.79 (1 H, d, *J* 8, H^3), 4.76 (2 H, br s, H^{23}), 4.63 (2 H, s, H^7), 4.24 (2 H, q, *J* 7, H^9), 4.21 (4 H, s, H^{11}), 4.19 (4 H, q, *J* 7, H^{13}), 1.29 (3 H, t, *J* 7, H^{10}), 1.25 (6 H, t, *J* 7, H^{14}); ^{13}C NMR (176 MHz, $CDCl_3$) 170.9 (C^{12}), 168.4 (C^8), 148.7 (C^1), 141.0 (C^2), 131.3 (C^{19} or C^{21}), 128.3 (C^{19} or C^{21}), 126.8 (C^4), 118.9 (C^3), 117.5 (C^6), 66.2 (C^7), 61.33 (C^9), 60.89 (C^{13}), 53.8

(C^{11}),14.2 (C^{14}), 14.1 (C^{10}); ESI-LRMS $[C_{26}H_{31}N_2O_8]^+$ (+) *m/z* 499.2; ESI-HRMS calc. for $[C_{26}H_{31}N_2O_8]^+$ 499.2080 found 499.2080.

*Protons from the pyridine ring system were very broad, and carbons (C^{18}, C^{19}, C^{20}, C^{21} and C^{22}) were not observed in the spectrum.

Diethyl 2,2'-((4-((2-(bromomethyl)pyridin-4-yl)ethynyl)-2-(2-ethoxy-2-oxoethoxy) phenyl)azanediyl)diacetate, (3)

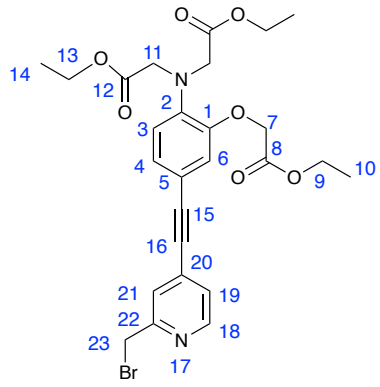

Phosphorus tribromide (PBr_3) (71 μL, 0.75 mmol) was added to an ice-cold solution of (**2**) (338.3 mg, 0.68 mmol) in anhydrous CH_2Cl_2 (6 mL). The reaction was warmed to room temperature and stirred at room temperature for 1 h under argon. Reaction completion was determined by LC-ESMS. The solvent was removed under reduced pressure to form a pale brown oil which was used without further purification. ESI-LRMS $[C_{26}H_{30}N_2O_8{}^{79}Br]^+$ (+) *m/z* 561.1; ESI-HRMS calc. for $[C_{26}H_{30}N_2O_8{}^{79}Br]^+$ 561.1238 found 561.1241.

Triethyl-2,2',2''-(10-((4-((4-(bis(2-ethoxy-2-oxoethyl)amino)-3-(2-ethoxy-2-oxoethoxy)phenyl)ethynyl)pyridin-2-yl)methyl)-1,4,7,10-tetraaza-cyclododecane-1,4,7-triyl)triacetate, (4)

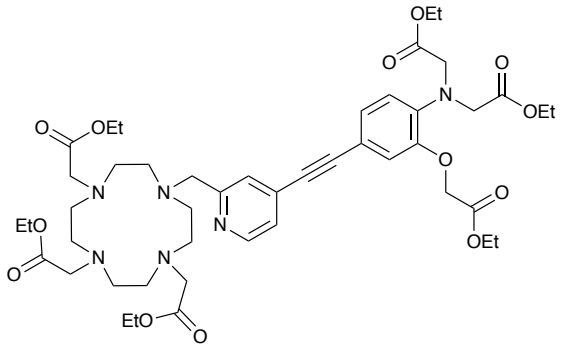

Caesium carbonate (632.4 mg, 1.94 mmol) and sodium iodide (73.8 mg, 0.49 mmol) were added to a solution of (**3**) (154.1 mg, 0.275 mmol) and [1,4,7-tris(ethoxycarbonylmethyl)]-1,4,7,10-tetraazacyclodecane hydrobromide (139.2 mg,

0.273 mmol) in anhydrous acetonitrile (3 mL). The reaction mixture was stirred at 60 C for 16 h under argon. The suspension was diluted with ethyl acetate (20 mL), and inorganic salts were removed by filtration. The solvent was removed under reduced pressure to give a dark brown residue. Purification by silica gel column chromatography (gradient 100 % CH_2Cl_2 to 90 % CH_2Cl_2 / 10 % MeOH) gave a pale yellow oil (160 mg). ESI-LRMS $[C_{46}H_{66}N_6O_{13}]^+$ (+) *m/z* 910.9; ESI-HRMS calc. for $[C_{46}H_{66}N_6O_{13}]^+$ 911.4766 found 911.4774.

EuL^1(H_2O)

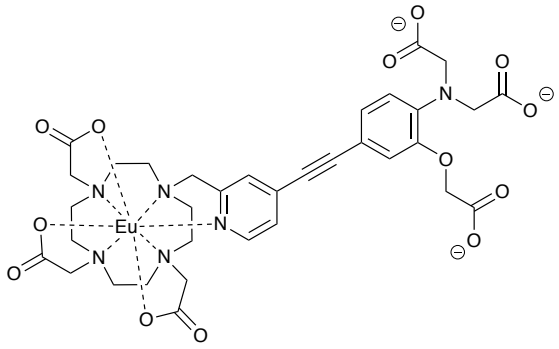

Compound (**4**) (64.3 mg, 0.07 mmol) was dissolved in CD_3OD (3 mL) and NaOD (0.4 M in D_2O, 0.80 mL). The pale yellow solution was stirred under an inert atmosphere of argon at room temperature for 18 h, ester hydrolysis was confirmed by ^{1}H NMR spectrometry and ESI-LRMS. The solution was lyophilised to yield the title compound as a white solid (61 mg), which was used in subsequent steps without further purification. ESI-LRMS $[C_{34}H_{43}N_6O_{13}]^+$ (+) *m/z* 743.2. The hydrolysed product of (**4**) (61.4 mg, 0.029 mmol) was dissolved in H_2O (3 mL) and the pH adjusted to 5.5 using HCl (aq, 1 M) and $EuCl_3.6H_2O$ (42.8 mg, 0.12 mmol) was added. The resulting yellow solution was stirred at 65 C for 18h, under argon. The pH was adjusted to 8 and the precipitated $Eu(OH)_3$ was removed by syringe filtration. Purification was achieved by reverse phase HPLC (0 % - 100 % - 0% CH_3CN in ammonium bicarbonate buffer (25 mM), t_R = 1.13 min). The solvent was lyophilised to afford the a pale yellow solid (13 mg); ESI-LRMS $[C_{46}H_{39}N_6O_{13}{}^{151}Eu]^-$ (-) *m/z* 890.3; ESI-HRMS calc. for $[C_{46}H_{39}N_6O_{13}{}^{151}Eu]^+$ 890.1774 found 890.1767; Φ_{H_2O}= 13.0 %.

Conflicts of interest The authors declare no conflicts of interest.

Acknowledgements We thank the EPSRC (EP/ L01212X/1) for generous support.

Key Words Magnesium; europium, terbium luminescence; selectivity; sensing.

References

[1] E. Soini and I. Hemmilla, *Clin. Chem*. 1979, **25**, 353-361.

[2] A. T. Frawley, R. Pal and D. Parker, *Chem. Commun*., 2016, **52**, 13349-13352.

[3] O. Reany, T. Gunnlaugsson and D. Parker, *J. Chem. Soc., Perkin Trans. 2*, 2000, 2, 1819-1831.

[4] O. Reany, T. Gunnlaugsson and D. Parker, *Chem. Commun*, 2000, 473-474.

[5] R. H. Laye and S. J. A. Pope, *Dalton Trans*., 2006, 3108-3113.

[6] A. K. R. Junker, M. Tropiano, S. Faulkner and T.J. Sørensen, *Inorg. Chem*., 2016, 55, 12299-12308.

[7] Y. Bretonniere, M. J. Cann, D. Parker and R. Slater, *Org. Biomol. Chem*., 2004, **2**, 1624.

[8] S. J. Butler, *Chem. Commun*., 2015, **51**, 10879-10882.

[9] A. M. P. Romani, Arch. *Biochem. Biophys*., 2011, **512**, 1-23.

[10] M. Tilmann, F. Wolf, *Curr Opin Pediatr*., 2017, **29**, 187-198.

[11] A. Romani and A. Scarpa, *Arch. Biochem. Biophys*., 1992, **298**, 1-12.

[12] B. Raju, E. Murphy, L. A. Levy, R. D. Hall and R. E. London, *Am. J. Physiol*., 1989, **256**, 540-548.

[13] P. A. Otten, R. E. London and L. A. Levy, *Bioconjugate Chem*., 2001, **12**, 76-83.

[14] M. S. Afzal, J-P. Pitteloud, D. Buccella, *Chem. Commun*., 2014, **50**, 11358-11361.

[15] Q. Lin, J. J. Gruskos and D. Buccella, *Org. Biomol. Chem*., 2016, **14**, 11381-11388.

[16] G. Zhang, J. J. Gruskos, M. S. Afzal and D. Buccella, *Chem. Sci*., 2015, **6**, 6841.

[17] F. L. Bygrave, A. Benedetti, *Cell Calcium*, 1996, **19**, 547-551.

[18] P. A. Otten, R. E. London and L. A. Levy, *Bioconjugate Chem*., 2001, **12**, 203-212.

[19] H. Komatsu, N. Iwasawa, D. Citterio, Y. Suzuki, T. Kubota, K. Tokuno, Y. Kitamura, K. Oka and K. Suzuki, *J. Am. Chem. Soc*., 2004, **126**, 16353-16360.

[20] S. C. Schwartz, B. Pinto-Pacheco, J-P. Pitteloud and D. Buccella, *Inorg. Chem.,* 2014, **53**, 3204-3209.

[21] E. R. H. Walter, M. A. Fox, D. Parker and J. A. G. Williams, *Dalton Trans,* 2018, **47**, 1879.

[22] E. R. H. Walter, D. Parker and J. A. G. Williams, *Chem. Eur. J.* 2018, doi: 10.1002/chem.201800013

[23] E. R. H. Walter, D. Parker and J. A. G. Williams, *Chem. Commun*. 2017, **53**, 13344-13347.

[24] K. Nakamaru, *Bull, Chem. Soc. Jpn*., 1982, **55**, 2697-2705.

[25] B. Gelerent, A. Findeisen, A. Stein and J. A. Poole, *J. Chem. Soc. Faraday Trans II*., 1973, **70**, 939.

[26] M. Soulié, F. Latzko, E. Bourrier, V. Placide, S. J. Butler, R. Pal, J. W. Walton, P. L. Baldeck, B. Le Guennic, C. Andraud, J. M. Zwier, L. Lamarque, D. Parker and O. Maury, *Chem. Eur-J.,* 2014, **20**, 8636-8646.

[27] M. Starck, R. Pal and D. Parker, *Chem. Eur- J.,* 2016, **22**, 570-580.

[28] G. Schreckenbach, *Chem. Eur. J.* 2017, **23**, 3797-3803.

[29] T. Riis-Johannessen, N. D. Favera, T. K. Todorova, S. M. Huber, L. Gagliardi and C. Piguet, *Chem. Eur. J.* 2009, **15**, 12702-12718.

[30] D. G. Smith, R. Pal and D. Parker, *Chem. Eur-J*., 2012, **18**, 11604-11613.

[31] R. Pal, L. C. Costello and D. Parker, *Org. Biomol. Chem*., 2009, **7**, 1525-1528.

[32] R. Pal, A. Beeby and D. Parker, *J. Pharmaceut. Biomed. Anal*., 2011, **56**, 352-358.

[33] L. M. Resnick, *Am. J. Hypertens*., 1993, 6, 123S-134S.

[34] A. Tin and M. E. Grams, *Kidney Int*., 2015, 820-827.

[35] www.supramolecular.org